IOP PUBLISHING JOURNAL OF PHYSICS B: ATOMIC, MOLECULAR AND OPTICAL PHYSICS

J. Phys. B: At. Mol. Opt. Phys. **41** (2008) 045301 (6pp) doi:10.1088/0953-4075/41/4/045301

Simulation of a strong van der Waals blockade in a dense ultracold gas

J V Hernández and F Robicheaux

Department of Physics, Auburn University, AL 36849-5311, USA

E-mail: hernajv@auburn.edu

Received 16 November 2007, in final form 26 December 2007
Published 11 February 2008
Online at stacks.iop.org/JPhysB/41/045301

Abstract

We report on simulations involving the blockade effect on a dense ultracold gas. The blockade effect is seen when the interaction energy between two excited Rydberg atoms is large enough to shift the two-excitation state out of resonance. In this paper we investigate a system that exhibits a strong van der Waals blockade, where only one out of thousands of atoms can be excited per blockade volume. With such a high number of atoms blockaded, the collective oscillation rate of an ensemble of atoms is much faster than the single atom oscillation rate. We examine the effects of this high density and the effects of a non-uniform density distribution as commonly seen in a magneto-optical trap (MOT). We use three different models and compare them to recent experimental data. The agreement between theory and experiment, although qualitative, suggests that the non-uniformity of the density within a blockade region presents a new challenge to theoretical models.

1. Introduction

The properties of an ultracold Rydberg gas have been the topic of several experimental and theoretical studies. If an ultracold gas of Rydberg atoms is cold and dense enough, the effect of the motion of the atoms is small compared to the possibly large interactions between them. Since Rydberg atoms are large in size, they are able to support large dipole moments. The relatively strong and long range interactions between dipole moments should dominate the physics in this dense ultracold regime, making it possible to study interesting many-body effects in detail. One such effect is seen when the interaction energy between Rydberg atoms is large enough to shift multiply excited states out of resonance with a tightly tuned excitation laser. With the multiple excitation states now blocked from occurring, the number of atoms able to be excited is suppressed. This suppression in the number of excited atoms is known as the blockade effect [1].

The dipole blockade effect was first described in [2] as a method of controlling and operating quantum logic gates. The process described in that proposal utilized the interactions between electric-field-induced dipoles and has been experimentally verified to produce a dipole blockade [3]. In [1] the proposed interaction was between Rydberg atoms at Förster resonance and a successful dipole blockade has been observed for this configuration as well [4]. A blockade using the second-order van der Waals interaction has also been experimentally seen [5–8].

The theoretical study of the dipole blockade effect must be able to take into account the many-body nature of the system. The effect of many bodies has been modelled using a mean field [5], a Monte Carlo approach [3, 9, 10], a perturbative approach [11] and by numerically solving the many-body wavefunction [12, 13]. Unless otherwise noted, atomic units will be used throughout this paper.

2. Theory

We report on calculations regarding Rydberg excitation of highly dense ultracold atoms. We simulated the physical set-up similar to [6]. In that experiment, a two-photon excitation scheme is employed from the $5S_{1/2}$ to $5P_{3/2}$ and finally to $43S_{1/2}$. Due to a large detuning to the blue on the $5S_{1/2}$ to $5P_{3/2}$ transition the three levels can be reduced to an effective two-level system [6]. So for all intents and purposes, we will consider each atom as a strictly two-level system: a tightly bound, non-decaying ground state, $|g\rangle$ ($5S_{1/2}$), and an excited Rydberg state, $|e\rangle$ ($43S_{1/2}$). The atoms are excited by a narrow bandwidth laser which is quickly and smoothly switched on for an excitation time, $\tau < 20\ \mu$s. The relevant time scales of the system are determined by comparing the linewidth of excitation to the interaction energy between Rydberg atoms. In

previous work [5, 12, 13], the bandwidth of the laser dominated the linewidth of excitation and therefore tied the time scale to the shape of the laser pulse. In this paper, the bandwidth of the laser is much smaller than the power broadening which is determined by the collective Rabi oscillations [6]. As in the experiment, we will take the density distribution of ground-state atoms to be Gaussian:

$$\rho(r, x, y, z) = \rho_0 \, \mathrm{e}^{-(x^2+y^2)/\sigma^2 - z^2/\Delta z^2}, \tag{1}$$

where ρ_0 is the peak density, $\sigma = 12$ μm is the width in the radial direction and $\Delta z = 220$ μm is the width in the axial direction. Since the peak density of the gas is quite high ($\rho \sim 3 \times 10^{12}$ cm^{-3}) and the van der Waals interaction between excited Rydberg atoms can be very large ($C_6 \propto n^{11}$), including many-body effects is important.

In this paper we take into account three interactions: the interaction of the laser on the atoms, the van der Waals interaction between two excited Rydberg atoms and a mean field energy shift between an excited Rydberg atom and excited Rydberg atoms outside of the simulated box. In order to reduce edge effects of the box and hasten convergence we also used wrap boundary conditions to calculate the interactions between atoms. The experimental set-up in [6] was able to cool the gas to 3.4 μK. At such a low temperature, the motion of the atoms is still small compared to the distances between Rydberg atoms. For example, at this temperature and at a density of 2.8×10^{12} cm^{-3}, after 20 μs the typical distance travelled by a Rb atom is 0.6 μm; while the distance between Rydberg atoms due to the blockade effect is about 5 μm. We therefore fixed the atoms in space.

2.1. The many-body wavefunction

In order to solve the many-body wavefunction for this system we expanded the wavefunction:

$$|\Psi(t)\rangle = a_{gg\ldots g}(t)|gg\ldots g\rangle + a_{eg\ldots g}(t)|eg\ldots g\rangle + \cdots + a_{ee\ldots g}(t)|ee\ldots g\rangle + a_{ee\ldots e}(t)|ee\ldots e\rangle \tag{2}$$

$$= \sum_\alpha a_\alpha(t)|\alpha\rangle. \tag{3}$$

As it would be impractical to attempt to include every single basis state in our expansion, we used a pseudoparticle approach to reduce the number of basis states very similar to [12]. These pseudoparticles have an interaction strength with the laser $\sqrt{W}$ times bigger than the single atom case, where the weight W is the number of atoms in each pseudoparticle. In [12], real atoms (pseudoparticles with weight equal to one) were randomly placed within a volume large enough to cover the region of correlation and then these strongly blockaded atoms were recursively grouped together to form pseudoparticles until the number of real atoms, N_a, is reduced down to the desired number of pseudoparticles. The recursion was as follows: (1) the nearest neighbours j and k were found, (2) these two 'atoms' were joined and replaced by a pseudoparticle i located at the centre of mass position $\vec{r}_i = (W_j\vec{r}_j + W_k\vec{r}_k)/(W_j + W_k)$, still making use of the wrap boundaries and (3) set the weight of the created pseudoparticle to $W_i = W_j + W_k$ while removing j and k from the simulation. The errors created by forcing correlations between atoms can be controlled by increasing the number of pseudoparticles. When the number of atoms, N_a, is low, the N_a^2 nature of the recursion is not significant when it comes to computing time. However, when N_a gets into the thousands needed to simulate densities along the lines of [6], using that recursion relation becomes computationally taxing. We took an alternate approach by using a Sobol sequence to place the pseudoparticles first. The Sobol sequence is a quasi-random sequence that fills space in more uniform manner than uncorrelated random points [14]. It avoids the clumpiness that occurs when filling a space with a random sequence, thus leading to quicker convergence. Once the pseudoparticles are placed, we generate a random position for an atom and, using wrapped boundary conditions, find which pseudoparticle it is closest to. The weight W of that pseudoparticle is then increased by one and the process is repeated until all of the atoms have been accounted for. There will now be a Poissonian distribution of atoms per pseudoparticle.

The interaction between excited pseudoparticles j and k can be calculated by averaging over all of the pairs of associated atoms:

$$V_{jk} = \frac{1}{W_j W_k} \sum_{n\in j} \sum_{m\in k} -\frac{C_6}{r_{nm}^6}, \tag{4}$$

where r_{nm} is the distance between atoms n and m, which belong to pseudoparticles j and k, respectively. Another way to calculate the interaction would be to simply use the positions of the pseudoparticles themselves, $V_{jk} = -C_6/r_{jk}^6$. Clearly, as the number of pseudoparticles is increased the two different methods will give the same interaction energies. We used the latter approach in our calculations because it converged faster with respect to random geometries as long as enough pseudoparticles were used.

If we assume that the initial state in every atom is the tightly bound ground state, $|\Psi(0)\rangle = |ggg\ldots g\rangle$, and we use the rotating wave approximation, then the Hamiltonian of the system can be written as follows:

$$\hat{H} = \sum_j \hat{H}_j^{(1)} + \sum_{j<k} V_{jk}|e_j e_k\rangle\langle e_j e_k|$$

$$\hat{H}_j^{(1)} = [-\Delta\omega(t) + \varepsilon(t)]|e_j\rangle\langle e_j| + \mathcal{F}(t)\frac{\Omega_0}{2}\sqrt{W_j}(|g_j\rangle\langle e_j| + |e_j\rangle\langle g_j|), \tag{5}$$

where $V_{jk} = -C_6/r_{jk}^6$ is the two-particle interaction between pseudoparticles j and k. The $43S_{1/2}$ state has a repulsive van der Waals interaction ($C_6 = -1.67 \times 10^{19}$).[1] The detuning of the laser is $\Delta\omega(t)$, and $\varepsilon(t)$ is a mean field energy shift due to a uniform distribution of excited atoms outside of the simulated volume. For the van der Waals potential, $\varepsilon(t) \simeq -f(t)20C_6\rho L^{-3}$, where $f(t)$ is the fraction of atoms excited and L^3 is the volume size [12]. The single atom Rabi frequency between states $|g\rangle$ and $|e\rangle$ is Ω_0 and the number of

[1] We calculated the value of this C_6 coefficient by using second-order perturbation theory and quantum defect theory. The necessary wavefunctions were generated by direct numerical integration in the radial direction using the quantum defects given by [15] and the resulting C_6 was in good agreement with [16].

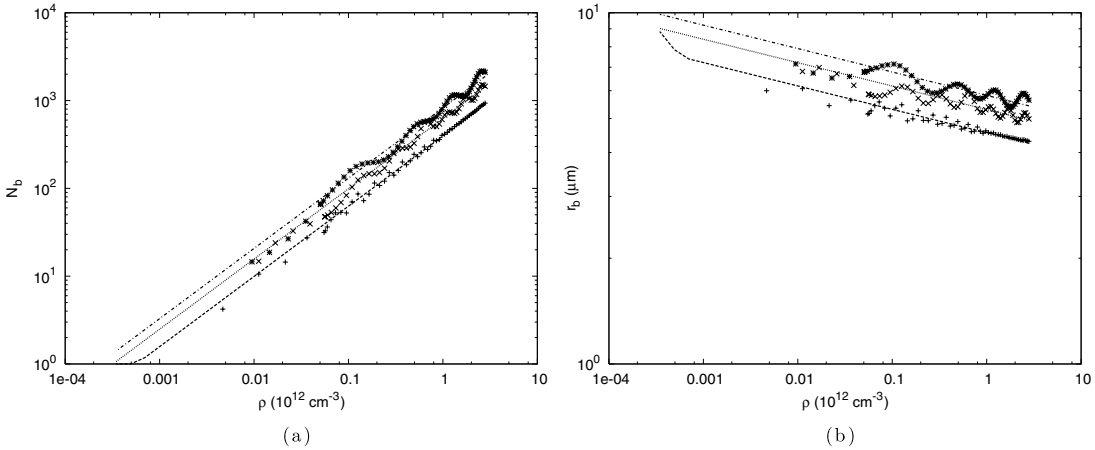

Figure 1. (a) The number of blocked atoms per excited atom, N_b, as a function of the density at various Ω_0. (- - - -, +) $\Omega_0 = 210$ kHz, ($\cdots\cdots$, $\times$) $\Omega_0 = 210/\pi$ kHz and (— · —, *) $\Omega_0 = 210/(2\pi)$ kHz. The lines were generated using the fact that $N_b \propto \rho^{4/5}$ and the points were generated by the many-body wavefunction at $\tau = 20$ μs. (b) The blockade radius, r_b, as a function of the density at the same Ω_0's as part (a).

atoms in each pseudoparticle, j, is W_j. The time dependence of the shape of the laser is described by

$$\mathcal{F}(t) = \begin{cases} e^{-25(t-t_r)^4/t_r^4} & \text{for} \quad t < t_r \\ 1 & \text{for} \quad t_r \leqslant t \leqslant \tau, \end{cases} \tag{6}$$

where $t_r = 100$ ns $\ll \tau$ is the ramp-on time and τ is the excitation time.

In order to solve the time-dependent Schödinger's Equation, we used the split operator method to propagate the initial wavefunction forward in time:

$$|\Psi(t+\delta t)\rangle = e^{-i\hat{H}_{off}(t)\delta t/2}\, e^{-i\hat{H}_{diag}\delta t}\, e^{-i\hat{H}_{off}(t)\delta t/2}|\Psi(t)\rangle. \tag{7}$$

We then used the many-body wavefunction to calculate the number of atoms excited, N_{exc}, and thus the fraction of atoms excited, $f(\tau) = N_{exc}(\tau)/N$, as a function of the excitation time.

3. van der Waals blockade

An atom can be considered 'blockaded' when the two-particle van der Waals interaction shifts the doubly excited state out of resonance, $C_6/r^6 > \Omega$. The interaction distance at which this occurs is called the blockade radius, $r_b \sim (C_6/\Omega)^{1/6}$. An ensemble of N_b blockaded atoms oscillates between a ground state and a symmetrical state with one excitation at the frequency $\Omega = \sqrt{N_b}\Omega_0$. At high densities the number of atoms blocked per excited atom, N_b, is large and closely follows a Poissonian distribution. When N_b is small, this increase in frequency is not significant; as $\sqrt{N_b}$ grows large, this effect becomes more important. A simple estimation of N_b depends on the local density and the volume that encloses the ensemble: $N_b \propto \rho r_b^3$. In order to estimate r_b, the number of blockaded atoms must be found. For an ensemble of N_b blockaded atoms, $r_b \propto (C_6/\sqrt{N_b}\Omega_0)^{1/6}$. In turn, an excited atom blocks all other atoms within a spherical volume $(4/3)\pi r_b^3$, so for a uniform distribution ρ, $N_b \propto (4/3)\pi r_b^3 \rho$. These two equations can be solved leading to $r_b \propto \rho^{-1/15}$ and $N_b \propto \rho^{4/5}$. The plots in figure 1 are the results for r_b and N_b as a function of density for ranges which are similar to those found in the MOT used by [6]. The lines were generated by the following equation:

$$N_b = \alpha \left(\frac{4\pi}{3} \sqrt{\frac{C_6}{\Omega_0}} \rho \right)^{4/5}, \tag{8}$$

where α is a fit parameter to match the data generated by the many-body wavefunction calculations. We used an $\alpha = 1.075$. As expected, as the density increases, r_b decreases and the N_b increases. The size of r_b is dependent on the local density. The oscillations in the numerical data are a result of treating each point as a 'perfect' experiment with a constant density and reading the fraction excited after exactly 20 μs. Since the collective Rabi frequency is related to the local density, taking the final reading always at 20 μs will pick the fraction excited at different points along the oscillation. The difference in r_b from the lowest density edges of the MOT to the peak density in the centre is substantial. The difference in N_b from peak to edge densities is also quite large, which means that excited atoms on the edges of the MOT will oscillate many times slower than ones near the centre. We introduce a scaled distance $\xi = \sqrt{r_c^2/\sigma^2 + z^2/\Delta z^2}$ from the centre of the MOT to study the spacial locations of the excitations within the MOT. The plots in figure 2 are the N_{exc} in a volume $4\pi\xi^2\Delta\xi$, where $\Delta\xi \ll \xi$, and N_b at given scaled distance ξ. Most of the excited atoms occur at about $\xi = \sqrt{5}$, which is about 6.7×10^{-3} times the peak density. The plot in figure 2(b) is both N_b and N_{exc} and a function of ξ. As the atoms are found further from the centre of the MOT the number of excited atoms per volume generally increases and the number of atoms that are blocked greatly decreases from N_b at the peak density. At $\xi = 0$, $N_b \sim 10^3$, while at $\xi = \sqrt{5}$, $N_b \sim 10$ which means the majority of the oscillations in the system will be about a factor of 10 times slower than oscillations at the peak.

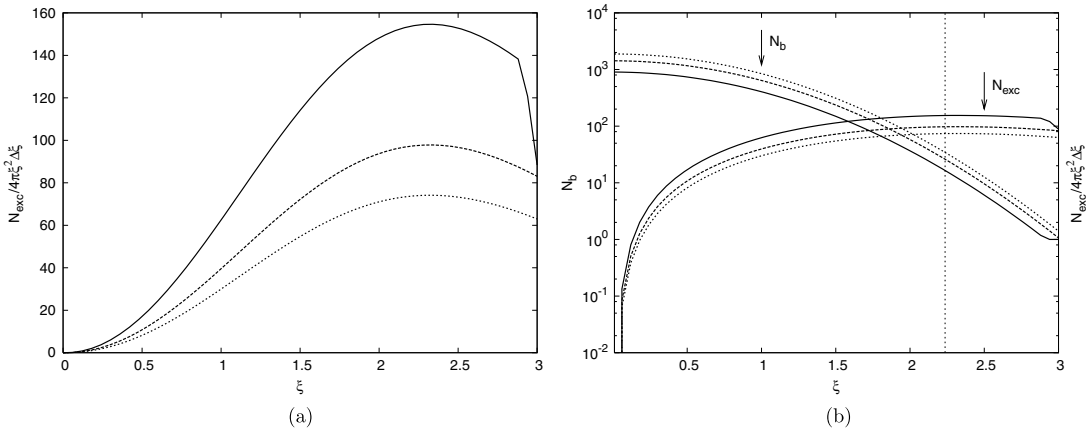

Figure 2. (a) The number of excited atoms $N_{\rm exc}$ in a volume $4\pi\xi^2\Delta\xi$ found at a scaled distance $\xi = \sqrt{r_c^2/\sigma^2 + z^2/\Delta z^2}$ from the centre of the MOT at various Ω_0. (——) $\Omega_0 = 210$ kHz, (- - - -) $\Omega_0 = 210/\pi$ kHz and (· · · · · ·) $\Omega_0 = 210/(2\pi)$ kHz. (b) $N_{\rm b}$ and $N_{\rm exc}/4\pi\xi^2\Delta\xi$ as a function of ξ. (——) $\Omega_0 = 210$ kHz, (- - - -) $\Omega_0 = 210/\pi$ kHz and (· · · · · ·) $\Omega_0 = 210/(2\pi)$ kHz. The vertical line is at $\xi = \sqrt{5}$, where $N_{\rm exc}/4\pi\xi^2\Delta\xi$ is maximum.

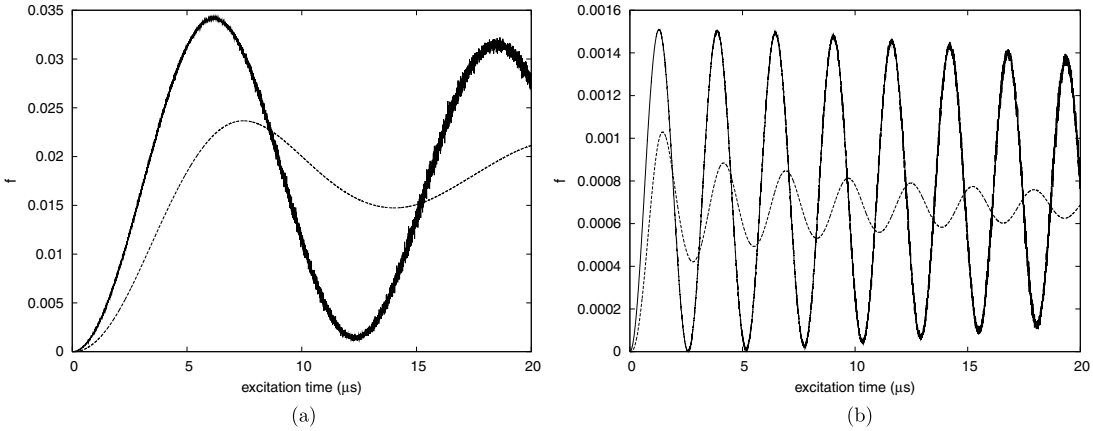

Figure 3. The fraction excited versus excitation time for the many-body wavefunction calculation (- - - -) and the simple $\sin^2$ model (——). (a) For a low density (5.6×10^{10} cm^{-3}) and (b) for a high density (2.8×10^{12} cm^{-3}). Both calculations were done using $\Omega_0 = 210/\pi$ kHz.

4. Effects of density variation

Even within a volume contained by $r_{\rm b}$, the density can vary enough to have an effect. For example, if $r_{\rm b} \sim 6$ μm, the diameter of a blockade is approximately σ. This means that density (and correspondingly $N_{\rm b}$) can vary by an order of magnitude within a blockade region. This variation in time scales and $r_{\rm b}$ indicates that in order to correctly model the entire gas the non-uniform density distribution of the MOT must be accounted for. In other words, the local fraction excited will depend on the local density, ρ, and the excitation time, τ. Unfortunately, the many-body wavefunction calculations utilize wrapped boundary conditions and a mean field in order to make convergence possible, both of which depend on a constant density across the simulated volume.

Given a density distribution, the total number of atoms excited to a Rydberg state after an excitation time, τ, will be

$$N_{\rm exc}(\tau) = \int f(\rho, \tau)\rho \, {\rm d}V, \tag{9}$$

where $f(\rho, \tau)$ is the fraction excited after excitation time τ for a density, ρ. We calculated $f(\rho, \tau)$ for various densities by solving the many-body wavefunction, but in these simulations we assumed that the density does not vary strongly within a blockade region. This condition does not hold up when using the parameters in [6] and will lead to a loss of accuracy in the calculations, but we still hoped for qualitative agreement with experiment. If, as in our case, the density distribution is Gaussian, this can be rewritten as

$$N_{\rm exc}(\tau) = 2\pi\sigma^2\Delta z \int f(\rho, \tau)\sqrt{\ln(\rho_0/\rho)}\, {\rm d}\rho. \tag{10}$$

In order to accurately integrate numerically over the density, we used a simple linear interpolation to get $f(\rho, \tau)$ for values between the calculated values. The accuracy of this integration is determined by the number of calculated density points and the grid size in density.

4.1. Simple sinusoidal model

As a check, we also developed a simple model based on the idea that a strongly blockaded ensemble of $N_{\rm b}$ atoms oscillates at $\sqrt{N_{\rm b}}\Omega_0$. For the large densities presented in this paper, the number of blockaded atoms for a certain density varies in a

Poissonian fashion from trial to trial. Using these criteria, an estimate of the fraction excited as a function of ρ and τ can be found:

$$f_{\rm est}(\rho,\tau) = \left\langle \frac{1}{N_{\rm b}(\rho)} \sin^2 \sqrt{N_{\rm b}(\rho)} \frac{\Omega_0}{2} \tau \right\rangle_{N_{\rm b}}, \qquad (11)$$

where the brackets, $\langle \cdots \rangle_{N_{\rm b}}$, indicate an average over a Poissonian distribution in $N_{\rm b}$. Figure 3 shows a comparison between the fraction excited versus time for the many-body wavefunction calculation and the simple sinusoidal model. The left figure is for a fixed relatively low density and the right is a fixed high density. This simple $\sin^2$ model assumes a perfect correlation between all atoms unlike the many-body wavefunction calculation which directly takes into account atoms outside of the region of strong correlation and a mean field energy shift caused by uncorrelated atoms outside of the simulated box. We wanted something that would give a good estimate for the oscillation time and also give a reasonable fraction excited for long excitation times. The lack of an additional damping mechanism other than the Poissonian average in the $\sin^2$ model is evident in the much higher contrast seen in the fraction excited. The oscillations in many-body wavefunction calculation are similar to the sinusoidal model, indicating the coherent nature of the system. The slight differences in oscillation times could also be explained by the crudeness of the sinusoidal model. At a higher density these oscillations are noticeably faster, but still coherent. If the density across the system does not drastically change, the collective Rabi oscillation is evident. If the density does change, the resulting high $\sqrt{N_{\rm b}}$ fluctuations will mask the collective excitations.

4.2. Monté Carlo model

Due to the small fraction of atoms excited to a Rydberg state, people have applied a Monte Carlo (MC) approach towards studying this system [10]. We used a very simple MC model that only allowed for excitations, no de-excitations. We started by randomly placing 15 000 000 atoms in a Gaussian distribution with the same parameters as above. For every time step, δt, each atom, j, has a probability of being excited given by

$$P_j = \frac{\pi}{2} \Omega_0 \frac{(\Omega_0/2)^2}{(\Omega_0/2)^2 + \bar{V}_j^2} \delta t, \qquad (12)$$

where $\bar{V}_j = \sum_k V_{jk} = \sum_k -C_6/r_{jk}^6$ is the energy shift between atom j and every other excited atom. $\bar{V}_j$ is updated every time a new atom has been excited. This MC model essentially blockades an atom if $|\bar{V}_j| \gg \Omega_0$ which is consistent with the spirit of the definition of being blockaded as previously described. The MC model has the advantage of not needing to be convolved, so it can serve as a quantitative check on the previous two methods.

The overestimation of the simple $\sin^2$ model is seen when we convolve the simple model over the density distribution as in figure 4, but the two calculations reach the saturation number of Rydberg atoms at about the same excitation time. We also compared the convolved data to recent experimental data [6].

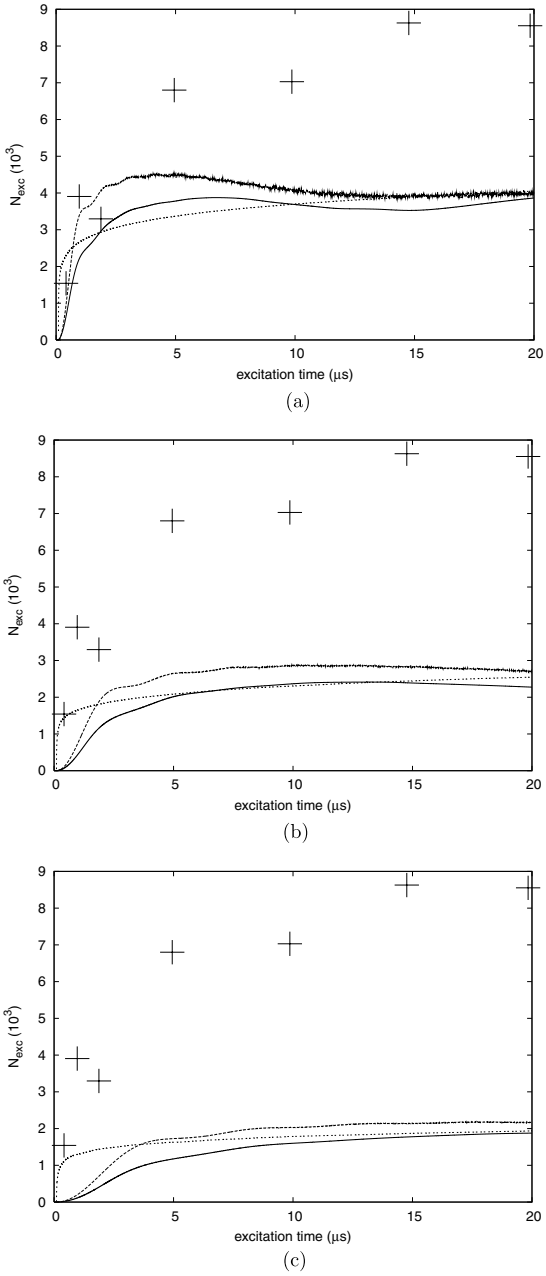

Figure 4. A comparison between the experimental data and the three models: the number excited versus excitation time for the convolved many-body wavefunction calculation (——), the simple $\sin^2$ model (- - - -) and the MC model (· · · · · ·). The (+) are experimental data points ($\Omega_0 = 210$ kHz). (a) Calculated using a Rabi frequency $\Omega_0 = 210$ kHz, (b) $\Omega_0 = 210/\pi$ kHz and (c) using $\Omega_0 = 210/(2\pi)$ kHz.

The experiment used a Rabi frequency of $\Omega_0 = 210$ kHz. The simulated result, while having the correct qualitative shape and within about a factor of 2 in the saturated number of excited atoms, is off when it comes to the time scale for saturation. We repeated these calculations using two slower Rabi frequencies in an attempt to match the time scale of the experiment. Unfortunately, as Ω_0 is decreased so does the $N_{\rm exc}$. This trend was consistent across all three models.

We could not perform a calculation that would match both the time dependence and the N_{exc} of the experiment with any of the available adjustable physical parameters. This suggests that only taking into account excited pair interactions and laser interactions while not accounting for a strong variance in density across a blockade region is not adequate enough to correctly understand this system.

5. Conclusion

We have performed three very different model calculations that are all in good qualitative agreement with each other. For such a large system of atoms, being within a factor of 2 in both time scale and N_{exc} is encouraging. However, the calculations do not agree well enough with experimental data to suggest that the underlying physics of the system is completely understood. The biggest concern is the different time scales for saturation between the computational models and the experimental data. Since we were not able to take into account the density variations over r_{b}, the first step towards developing a more accurate model might be to develop a method that can account for this density variance and also converge within feasible limits. This would present a challenge to any mean field calculations, as the value of the mean field energy shift would depend on the location of the pseudoparticle within the MOT. The actual shape of the gas is also very important if accurate models are to be developed since in all of the simulations the time scale is largely determined by the slower oscillations found towards the edges of the MOT where the density is lower.

Acknowledgment

This material is based upon work supported by the National Science Foundation under grant no 0355039.

References

[1] Lukin M D *et al* 2001 *Phys. Rev. Lett.* **87** 037901
[2] Jaksch D *et al* 2000 *Phys. Rev. Lett.* **85** 2208
[3] Vogt T *et al* 2007 *Phys. Rev. Lett.* **99** 073002
[4] Vogt T *et al* 2006 *Phys. Rev. Lett.* **97** 083003
[5] Tong D *et al* 2004 *Phys. Rev. Lett.* **93** 063001
[6] Heidemann R *et al* 2007 *Phys. Rev. Lett.* **99** 163601
[7] Liebisch T C *et al* 2005 *Phys. Rev. Lett.* **95** 253002
[8] Singer K *et al* 2004 *Phys. Rev. Lett.* **93** 163001
[9] Amthor T *et al* 2007 *Phys. Rev. Lett.* **98** 023004
[10] Ates C *et al* 2006 *J. Phys. B: At. Mol. Opt. Phys.* **39** L233
[11] Reinhard A *et al* 2007 *Phys. Rev.* A **75** 032712
[12] Robicheaux F and Hernández J V 2005 *Phys. Rev.* A **72** 063403
[13] Hernández J V and Robicheaux F 2006 *J. Phys. B: At. Mol. Opt. Phys.* **39** 4883
[14] Press W H *et al* 2007 3rd edn *Numerical Recipes* (Cambridge: Cambridge University Press)
[15] Li W *et al* 2003 *Phys. Rev.* A **67** 052502
[16] Singer K *et al* 2005 *J. Phys. B: At. Mol. Opt. Phys.* **38** S295